Geology and thermal history of the Pliocene Cerro Negro volcanic necks and adjacent Cretaceous sedimentary rocks, west-central New Mexico

R. Bruce Hallett, Philip E. Long, John Lorenz, and Bruce Bjornstad
1999, pp. 235-245. https://doi.org/10.56577/FFC-50.235

in:

Albuquerque Geology, Pazzaglia, F. J.; Lucas, S. G.; [eds.], New Mexico Geological Society 50 th Annual Fall Field Conference Guidebook, 448 p. https://doi.org/10.56577/FFC-50

This page is intentionally left blank to maintain order of facing pages.

GEOLOGY AND THERMAL HISTORY OF THE PLIOCENE CERRO NEGRO VOLCANIC NECK AND ADJACENT CRETACEOUS SEDIMENTARY ROCKS, WEST-CENTRAL NEW MEXICO

R. BRUCE HALLETT[1], PHILIP E. LONG[2], JOHN LORENZ[3], and BRUCE BJORNSTAD[4]

[1]Golder Associates Inc., 18 Santa Maria Dr., Edgewood, NM 87015; [2]Battelle-Pacific Northwest National Laboratory, MS K9-33, Richland, WA 99352; [3]Sandia National Laboratory, MS 0751, Albuquerque, NM 87185; [4]Battelle-Pacific Northwest National Laboratory, MSIN K6-81, Richland, WA 99352

Abstract—Two vertical and two angled boreholes were drilled through a Cretaceous–Jurassic section of shale and sandstone adjacent to the Pliocene Cerro Negro necks. One hundred fifty-seven meters of vertical and 575 m of angled core have been recovered, logged, and sampled to establish the section's sedimentologic, depositional, fracture, and thermal characteristics. Detailed core logging from ground surface to the top of the Brushy Basin Member of the Morrison Formation (Jurassic) generally supports published interpretations of depositional environments for this section. Geologic mapping at a scale of 1:2500 identifies a linear array of intrusive features that are roughly parallel to a regional NNE fracture/fault trend. Indirect evidence from drilling suggests the subsurface geometry of the Cerro Negro necks to be unlike the surface expression; additional drilling and geophysical studies will be necessary to map accurately the subsurface geometry. Fracture mapping in surface outcrop and core indicate two dominant, steeply dipping fracture trends, NNE, and a second roughly perpendicular trend of ESE. Although the Cerro Negro necks were not intersected in the angle holes, vitrinite data suggest a thermal aureole associated with the Cerro Negro intrusions of sufficient heat (>125°C) to sterilize local rocks in an approximate 50-m radius.

INTRODUCTION

Purpose and objective

The Department of Energy's (DOE) Subsurface Science, Deep Microbiology Subprogram supports basic research in the fields of microbial ecology and the origins of microbiota in deep sediments and aquifers with emphasis on survival and long distance transport of microbial communities over geologic time. The scientific drilling effort at Cerro Negro was a collaboration of geologists, hydrologists, geochemists, and microbiologists from numerous national laboratories, universities and research institutions assembled to investigate specifically in situ bacterial survival and mobility in a high temperature subsurface environment (Onstott, 1994; Fredrickson and Onstott, 1996).

Our research at Cerro Negro focused on a low-permeability, organic-rich marine shale, where transport of microorganisms was believed to be geologically retarded and where geologic and geochemical conditions were conducive to long-term survival. Cerro Negro was chosen as a drill site because of the opportunity to sample across shale/sandstone contacts over a short stratigraphic interval, a volcanic/thermal source of known age, and a reasonably well-understood geometry of the near surface volcanic intrusion. DOE supports this type of research, given the numerous industrial sites and military installations under their management, which have significant deep groundwater pollution, usually in the form of hazardous organic or metallic compounds, costing millions of dollars per year to remediate. Less expensive, nonintrusive biotechnologies that rely upon stimulation of the indigenous subsurface microbial communities may, over the long term, reduce remediation time, energy resources, and costs, compared to existing technologies.

Location

The Cerro Negro field site is located approximately 5 km east of the village of Seboyeta, in west-central New Mexico on land owned by the Cebolleta Land Grant (Fig. 1). Seboyeta is approximately 80 km west of Albuquerque. The Cerro Negro volcano is one of more than 50 volcanic necks in the Rio Puerco Valley (as a group, informally known as the Rio Puerco necks), which dot the margins of the late Tertiary Mount Taylor volcanic field (Hallett et al., 1997).

Previous geologic investigations

The earliest recorded geologic investigation and mapping in the Cerro Negro area was conducted more than a hundred years ago by U.S. Army officer and geologist Major Clarence E. Dutton (1884–85). Later, Johnson (1907) and Hunt (1937) produced more complete descriptions of the various landforms in the vicinity with detailed geologic maps. More recently, geochemical and petrographic studies (Brown, 1969; Aoki and Kudo, 1976; Hallett et al., 1997) have identified Cerro Negro

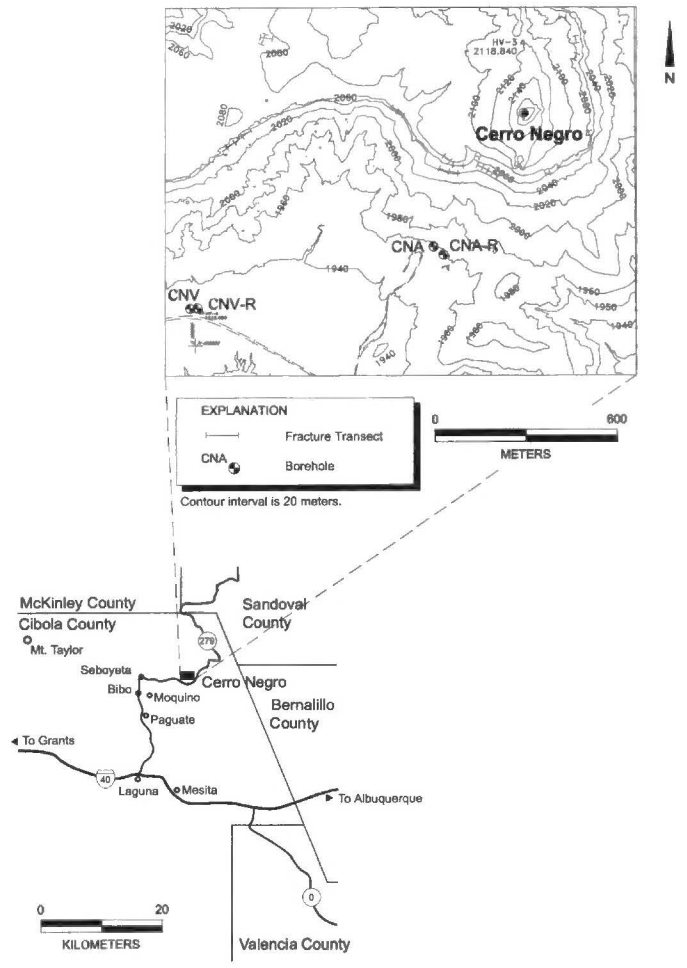

FIGURE 1. Location map of study area. Upper topographic map shows locations of boreholes and fracture mapping transects.

as being composed of alkali basalt with localized concentrations of mantle xenoliths (Brunton, 1952; Kudo et al., 1971; Wilshire et al., 1988).

The Laguna area (Fig. 1), located several kilometers south of Cerro Negro, became noteworthy for its uranium resources in the 1950s with the discovery of the Jackpile-Paguate deposit in 1951 (Saucier, 1979). Uranium ore was primarily mined from Jurassic continental, fluvial sediments during the 1950s to early 1980s. As a result of this mining/exploration effort a great deal was learned about the local tectonic history, structure, and sedimentation of Jurassic and Cretaceous rocks (e.g., Rautman, 1980; Turner-Peterson and Santos, 1986). In response to the economic interest in the area, the U.S. Geological Survey published a series of 7.5-minute geologic quadrangle maps and reports in the 1960s (e.g. Schlee and Moench, 1963; Moench and Schlee, 1967).

DRILLING, SAMPLING, AND MAPPING PROGRAM

Four boreholes (Fig. 1) were drilled at Cerro Negro in the Summer and Fall of 1994. Two vertical boreholes (CNV and CNV-R) were drilled 1.3 km southwest of the intrusions in order to establish vertical stratigraphy, sample groundwater, and conduct permeability tests. Two angled boreholes (CNA and CNA-R), about 0.45 km from the volcano, were drilled at a northeasterly azimuth toward the more southern plug of the volcanic center. These boreholes were located on a flat, 2023-m^2 drill pad as close as possible to the southern plug to minimize drilling costs. The stratigraphic intervals in which core were collected are shown in Table 1.

Continuous core samples were obtained using nitrogen and/or mud rotary drilling techniques. The core retrieval assembly consisted of a wireline-conveyed, 1.5-m core barrel with lexan liners and collected 6.35- and 8.89-cm diameter core. Pre-sterilized lexan liners were used to facilitate collection of core under sterile conditions for microbiological reasons. All core was either processed for microbiological analysis or logged and archived in core boxes at Pacific Northwest National Laboratory.

Air or nitrogen was used as the drilling fluid, where possible, to minimize contamination and minimize impact on in situ redox conditions, however, there were occasions when mud rotary was used to keep the core bit on azimuth in the angled hole (CNA-R). A number of innovative chemical and physical tracers (LiBr, microspheres, and perfluorocarbon) were incorporated into the sampling procedure in order to quantify ex situ microbial contamination (e.g., Colwell et al., 1992).

Detailed geologic mapping of Cerro Negro was undertaken to determine the number and types of volcanic features present. In addition, fractures were evaluated to determine the effects of fracture frequency and distribution in relation to proximity to the plug (Bjornstad et al., 1996). Fractures were measured in surface outcrops along 23 transects (Figs. 1, 2) at distances up to 1 km from the 180-m-wide volcanic intrusion, within two resistant Late Cretaceous units (Gallup Sandstone and Dilco Coal Member). Fractures were also observed and measured in CNV and CNA-R. Fracture properties were noted for orientation, width, and fracture-infilling material.

TABLE 1. Core recovered by stratigraphic interval. CNA and CNA-R depths have not been corrected to true vertical depth.

Stratigraphic interval	Borehole			
	CNV (m)	CNV-R (m)	CNA (m)	CNA-R (m)
Mancos Shale, "main body"	16.8¥	NR	66.5TD	249.0
Twowells Sandstone	22.8	NR	—	53.6
Whitewater Arroyo Shale	15.8	NR	—	28.9
Paguate Sandstone	22.9	NR	—	37.2
Clay Mesa Shale	9.1	5.5	—	15.2
Cubero Sandstone	13.0	11.7	—	18.6
Oak Canyon Sandstone	6.5TD	30.5	—	49.7
Jackpile Sandstone	—	2.2TD	—	21.3
Brushy Basin	—	—	—	66.3TD

NR - no recovery of core; hole advanced with tri-cone bit.
¥ - some portion of borehole advanced with tri-cone bit.
TD - total depth.

STRATIGRAPHY

Figure 3 is a composite stratigraphic section assembled from the 4 boreholes drilled at Cerro Negro. Angled borehole CNA-R reached a total vertical depth of about 305 m (511.8-m total intercept) in the Brushy Basin Member of the Morrison Formation, while the vertical borehole CNV-R reached a total vertical depth of 232.5 m in the Jackpile Sandstone of the Morrison Formation. The following lithologic description is derived from continuous core collected from about the middle of the main body of the Mancos Shale down to the Brushy Basin Member of the Morrison Formation.

Upper Jurassic strata

The Brushy Basin Member of the Morrison Formation is a greenish gray to brownish black mudstone with minor, thin occurrences of muddy sandstone. The sandstones are moderately sorted and silica cemented. Thin occurrences of reddish gray mudstone are common. Approximately 47.0 m of the upper Brushy Basin were drilled.

Above, and in depositional contact with the Brushy Basin, is the Jackpile Sandstone Member of the Morrison Formation, which consists of a light gray sandstone, with thin interbedded blue-green to greenish-gray siltstone and mudstone. The sandstones are fine-grained, moderately sorted, and moderately cemented with silica and/or clay. This unit is approximately 14.0 m thick and is known to thicken southward (Condon and Peterson; 1986). Owen (1982) estimates the unconformity between the Jackpile and Cretaceous rocks represents a 45-m.y. hiatus in deposition.

Upper Cretaceous strata

In previous outcrop investigations from the Laguna-Paguate area, the Oak Canyon Member of the Dakota has been divided into two units (Landis et al., 1973; Maxwell, 1982); a lower unit (basal of Maxwell, 1982) consisting largely of fluviatile and paralic sandstones and shale, and an upper unit consisting of paralic and marine sandstone and mudstone. These two different depositional units are recognized in the Cerro Negro boreholes, where the lower unit is dominated by cross-laminated, weakly cemented (calcite), muddy sandstone with occasional high concentrations of carbonaceous fragments and thin (2–10 mm) layers of coal. Soft sediment deformation structures and burrows are common, as is disseminated pyrite. One thin bentonite layer (<10 cm) occurs near the middle of the lower unit. The contact between the lower and upper parts is a sharp lithologic change marked by the first up-section occurrence of a thin, sideritic-oolite-rich muddy sandstone (lower) to a very well-sorted, glauconitic sandstone. The total thickness of the lower Oak Canyon is 8.5 m.

The upper Oak Canyon unit consists of calcite cemented, dark to medium gray muddy sandstones and grayish black sandy mudstones. The sandstones are moderately sorted and laminar to cross-bedded, and the mudstones are thinly laminated and bioturbated. Unlike the lower Oak Canyon, the upper part contains numerous thin-bedded, medium to dark gray, fossiliferous limestone layers. Two medium gray bentonite layers occur within the upper Oak Canyon, one near the base (~15 cm thick) and one near the top (~40 cm thick). Kaolinite, illite, and smectite were identified by x-ray fluorescence in all three bentonites (Elliott et al., 1999). The total thickness of the upper Oak Canyon is 21.5 m.

A gradational contact separates the Oak Canyon from the Cubero Sandstone. The Cubero is a calcite cemented, light gray to gray black, well-sorted, medium-grained sandstone with cross-laminations and bioturbated muddy and limy interbeds. Low-angle cross-bedding is common. Total thickness of the Cubero Sandstone is 13.0 m.

In depositional contact with the Cubero is the Clay Mesa Shale. This fine-grained unit contains numerous shell fragments and occasional pyrite. Laminar bedding throughout most of the Clay Mesa gives way to bioturbated beds in the upper few meters and continues over into the Paguate Sandstone Tongue. Total thickness of the Clay Mesa Shale is 9.1 m.

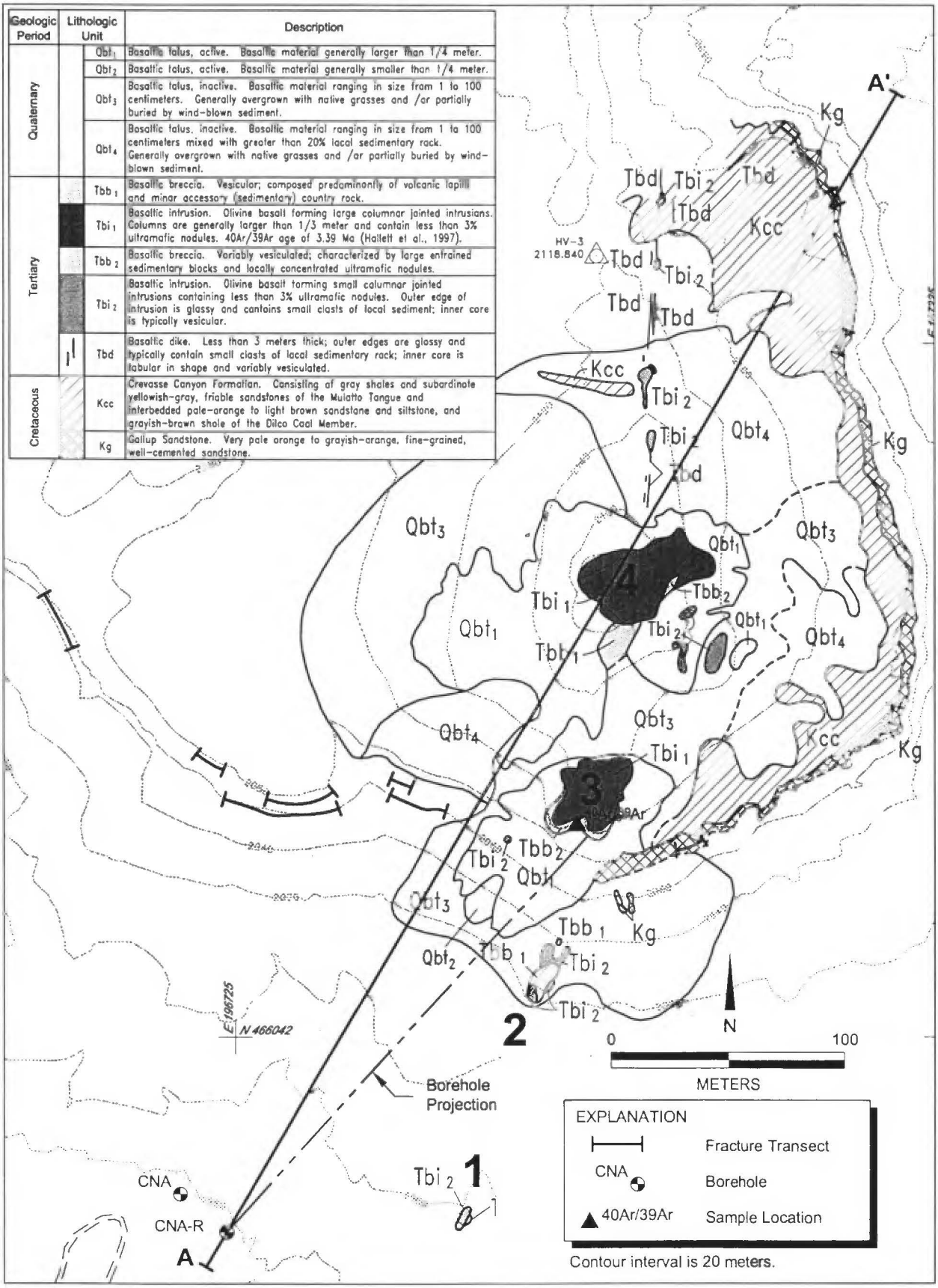

FIGURE 2. Geologic map of Cerro Negro. Sites mentioned in text shown with bold numbers. See Figure 8B for cross section along A–A'. The projected trace of angled borehole CNA-R is shown by the dashed line. The geologic legend shows relative age differences for Quaternary and Tertiary units based on mapping relationships.

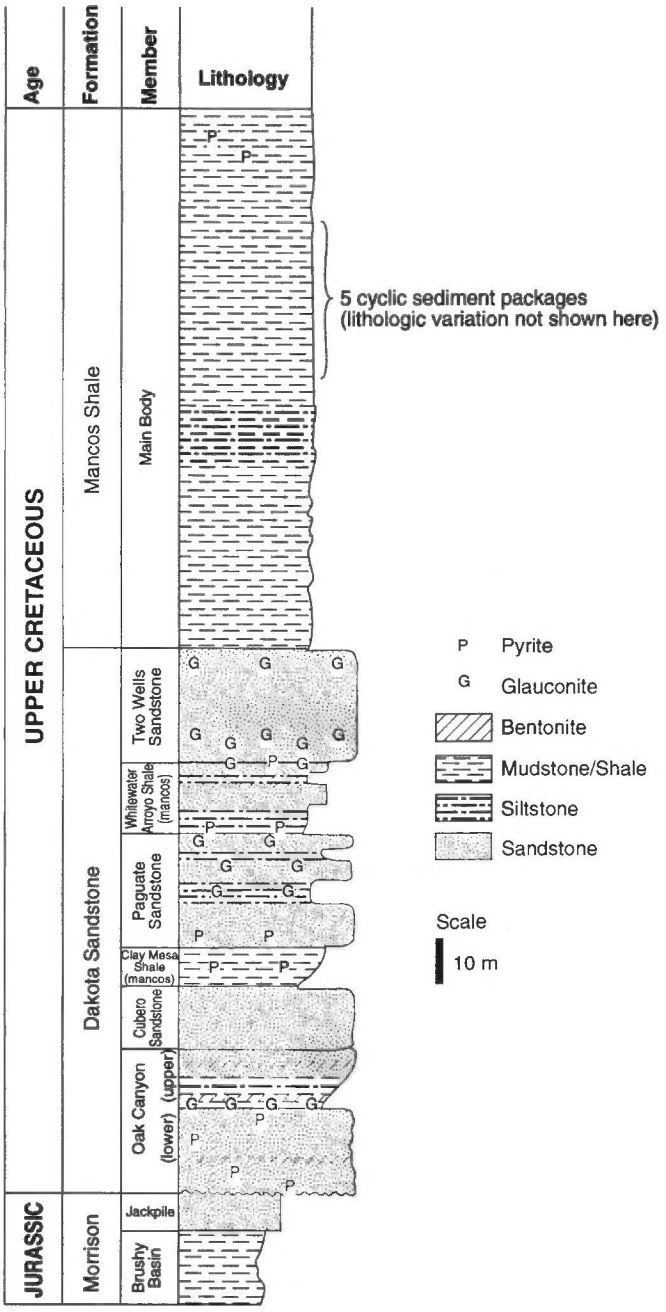

FIGURE 3. Composite stratigraphic section produced from boreholes CNV, CNV-R, CNA, CNA-R.

The Paguate Sandstone Tongue consists of alternating grayish black to light gray, limy and fine-grained, muddy sandstones. Each sandstone layer is well-sorted, calcite cemented, and laminated. Disseminated glauconite occurs throughout the upper two-thirds of this unit, particularly in the cleaner, sand-rich layers. Total thickness of the Paguate Sandstone is 22.9 m.

A gradational lithologic change from muddy sandstone to a sandy mudstone is observed at the Paguate/Whitewater Arroyo Shale contact. The younger Whitewater Arroyo is primarily a grayish black to olive black, moderately sorted, calcite-cemented, finely laminated and bioturbated siltstone. Two thin light gray bentonite layers containing kaolinite, smectite, and illite (Elliott et al., 1999) occur within the upper third of the unit. Total thickness of the Whitewater Arroyo Shale is 15.8 m.

The Twowells Sandstone Tongue of the Dakota lies above the Whitewater Arroyo Shale and consists of alternating medium-grained sandstone and silty sandstone. Generally, the sandstones are medium dark gray to dark gray, moderate to well sorted, and medium to fine grained. Dark, organic-rich, fine-grained laminations are common throughout the lower half of this unit and display variable bioturbation and soft sediment deformation. Disseminated glauconite is present in the more sand-rich intervals. As a whole, the Twowells displays a general coarsening upwards to a medium-grained sandstone. Total thickness of the Twowells Sandstone is 22.8 m.

The top Twowells/Mancos contact is marked by a discrete change from medium-grained sandstone to siltstone. Although the complete section of the main body was not drilled, there appears to be a series of discrete coarsening upward bedding packages (Fig. 3) which consist of one or several shale-mudstone couplets with minor sandstone on top. Mudstone and shales are grayish-black to dark gray, cross-laminated, bioturbated and calcite cemented. Shell fragments are common throughout the fine-grained intervals, as is disseminated pyrite. Sandstone layers are typically very well sorted, finely cross-laminated, bioturbated and calcite cemented. The total thickness of the drilled main body of the Mancos Shale is 115.1 m.

Basalt of Cerro Negro

Cerro Negro consists of five igneous features; two large plugs, two smaller plugs, and a series of discontinuous dikes (Fig. 2). The largest plug is identified as Cerro Negro on Figure 1 and by the number 4 on Figure 2, and the smaller of the large plugs is here referred to as the south plug (number 3, Fig. 2). Four basaltic dikes were intercepted at depth in the angled borehole near the south plug. Each is less than 1 m thick (true thickness) and intruded at subvertical angles with respect to nearly horizontal bedding planes. Thermal alteration to sedimentary units adjacent to the basaltic dikes is limited to slight discoloration that extends no more then 35 cm beyond the contact. In core, the basalt is grayish black, fine grained and vesicular. In outcrop the basalt is a black, non-vesicular, porphyritic olivine basalt. Olivine and clinopyroxene make up about 15% of the phenocryst phase; clinopyroxene, plagioclase, and opaques make up the groundmass. Cerro Negro has a $^{40}Ar/^{39}Ar$ plateau age of 3.39 ± 0.02 Ma (Hallett et al., 1997). It is assumed that the dikes encountered in CNA-R are the same age as Cerro Negro.

GEOLOGIC MAPPING

A geologic map at a scale of 1:2500 is shown in Figure 2. The five igneous features (four plugs and a series of discontinuous dikes) that make up Cerro Negro are oriented in a roughly linear N5°E trend. The largest plug (4 on Fig. 2) forms the crest of Cerro Negro. It reaches an elevation of 2201 m and has a mean basal diameter of 40 m. South plug (3 on Fig. 2) has an elevation of 2150 m and is more circular in shape, with a mean basal diameter of 30 m. Based on the surface expression of south plug, the angled boring CNA-R came very close to intersecting the plug at depth.

The southernmost igneous body (1 on Fig. 2) is a small, vertical intrusion 4 m in width. A chill zone about 10 cm wide on either side of the intrusion is vesiculated and contains small (<3 cm) subrounded, partially fused accessory lithics (sedimentary), similar in composition to sandstone of the Crevasse Canyon Formation (Kcc) and Gallup Sandstone (Kg). The interior of the intrusion is less vesiculated and contains 5% ultramafic xenoliths. Thin outcrops of basaltic breccia (Tbb2) are preserved on the eastern side of the intrusion.

Approximately 45 m to the northeast is another small intrusion (Tbi2; 2 on Fig. 3) and associated basaltic breccia (Tbb1). The outcrop dips very steeply to the northwest. On average, Tbb2 breccia is characterized by large entrained sedimentary blocks and locally concentrated ultramafic nodules. It is likely more explosive in origin than Tbb1, which is predominantly volcanic lapilli and minor accessory country rock. These breccias consist of scoriaceous basaltic lapilli and lesser amounts of accessory lithics. The breccias are pyroclastic in origin and are welded to form subvertical outcrops adjacent to the intrusive bod-

ies. There are no occurrences of volcanic bombs.

South plug (3 on Fig. 2) is composed of non-vesicular olivine basalt (Tbi1) with on average of less than 1% ultramafic xenoliths. Columnar jointing is irregular and mostly horizontal, except toward the upper regions where columns become curved skywards. On the east, south and west sides of the plug, are pyroclastic breccias (Tbb2) rich in accessory lithics. The breccias are less than 3 m thick with an internal appearance of a basaltic lava-sediment slurry. On the southeastern face of the plug is an exposure of pyroclastic breccia that covers an area of about 20 m^2 and is composed of about 40% ultramafic xenoliths. The breccia basalt is slightly vesicular but overall is similar in composition to the plug basalt.

The large plug to the north (4 on Fig. 2) is similar in composition to south plug but more regularly jointed. This plug appears to represent a single intrusion, but the surfaces through which heat was lost are quite complex as inferred from the jointing pattern. For example, jointing in the upper regions is slightly convex while further down the plug columns are nearly vertical and flaring at the base.

A 2-m-wide dike extends intermittently to the north of the plugs. It intermittently covers 300 m and disappears at the edge of the cliff formed by the Gallup Sandstone. Vesiculation in the dike decreases inward from the edges with little evidence of baking or disturbance of the adjacent country rock. It is assumed that all volcanic features at Cerro Negro erupted and/or were emplaced during a single volcanic event.

The two largest basaltic intrusive bodies (Tbi1) at Cerro Negro display columnar jointing greater than 1/3 m in diameter. Columnar jointing of non-vesicular basalt is a common feature of volcanic necks in this area (Hallett, 1992; Hallett et al. 1997). As magma cools, columnar joints form perpendicular to the conductive cooling surface and are the result of thermal stresses encountered during the cooling of the intrusion (Spry, 1962; Long and Wood, 1986). In small batches of magma (e.g., <10 m^3), heat is lost from the intrusion radially, thus producing a radial pattern of columns such as those seen in Cerro Negro. For example, the smaller intrusions (1 and 2 on Fig. 2) are typically jointed with columns less than 1/3 m in diameter. The outer edges of the intrusions are glassy and contain small clasts of local sediment. The inner core of the intrusion is commonly vesiculated. In larger necks (e.g., Cabezon Peak, New Mexico; Devils Tower, Wyoming), vertical columnar joints may form in the upper regions of the conduit as heat is lost through the top of the vent (e.g., horizontal surface of lava lake).

FRACTURE RESULTS

Measurement and analysis of fractures was done to assess the possible significance of fractures as conduits for microbial transport in the subsurface. Based on outcrop studies at Cerro Negro, Bjornstad et al. (1996) report that most are perpendicular to near horizontal bedding planes and restricted to more competent sandstones. In general, fractures were observed to terminate along interfaces with adjacent, less resistant beds (i.e., shales). Fractures are present in shale layers above and below sandstone beds, but are less abundant, less regular, and not as extensive. Two dominant fracture directions were observed (Fig. 4). The north-northeast-trending set (015° ± 15°) is predominant; the second set is roughly perpendicular to this set and is normally distributed around a mean trend of ESE (105° ± 15°). Most fractures are near-vertical (80–90° dip), extension-type fractures. Fractures are locally filled with secondary minerals, including calcite and iron oxide, in proximity to basaltic intrusions on the surface and near basalt dikes in the subsurface.

Fracture density in the Gallup Sandstone increases in proximity to the plug, with ranges from about 1 fracture per 10 m at a distance of 1000 m from the plug to 4 fractures per 10 m adjacent to the plug (Fig. 5). Within a few meters of the plug, fractures in the Gallup Sandstone are very irregular in orientation, and are filled with a white, powdery, calcitic material that is similar to the material found in association with what may have been a fumarole located north of the main plug on the west side of the dike. Otherwise, fracture orientation does not appear to vary with distance from the intrusion, and dip directions near the intrusion are the same as those farther away, suggesting a similar stress regime for the fractures and the intrusion.

Fracture analyses were also performed on core samples collected from CNV and CNA-R. Fracture orientations were reconstructed using the hole azimuth, hole deviation, and planar bedding surfaces, which were assumed to be horizontal. Fracture analyses of core indicated two trends, approximately north–south (predominant) and east–west, similar to fracture trends observed in outcrop. The low number of observed fractures in the angled borehole (CNA-R) were probably due to the near-parallel direction of the hole azimuth (NE) and the dominant fracture trend (NNE). For a similar reason, the vertical core from CNV did not display many fractures because most of the fractures are oriented vertically.

VITRINITE DATA

Procedure

Reflectance analyses were made on kerogen from 43 shale and sandstone samples (Table 2, Fig. 6) using standard rock preparation techniques (Mukhopadhyay and Dow, 1994) with kerogen isolation using density sink/float at 1.8 g/mL. When possible, 20 reflectance points were made on each sample using rotational polarization. The kerogen type used for reflectance measurement consists of vitrinite which represents material derived from woody plant precursors. Inertinite, or organic material derived from partially carbonized plant precursors, and

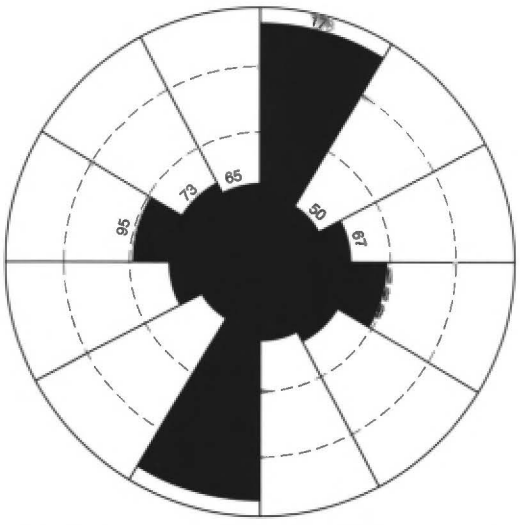

FIGURE 4. Rose diagram showing distribution of 528 separate fracture orientations from 23 transects in the Gallup Sandstone and Dilco Coal Member.

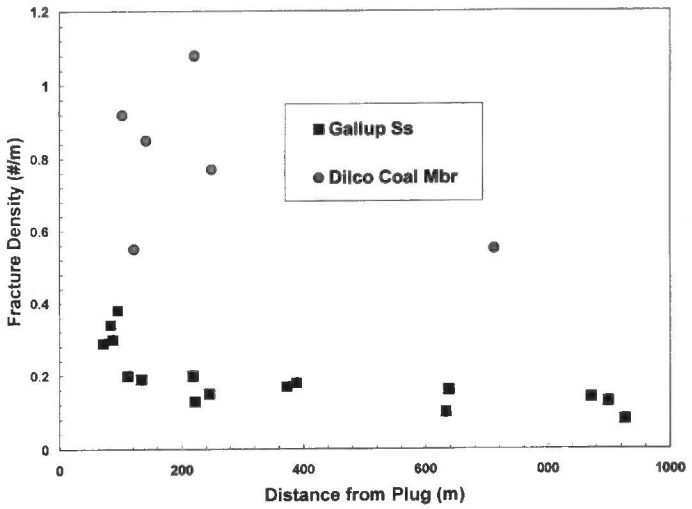

FIGURE 5. Plot showing fracture density in relation to distance from plug.

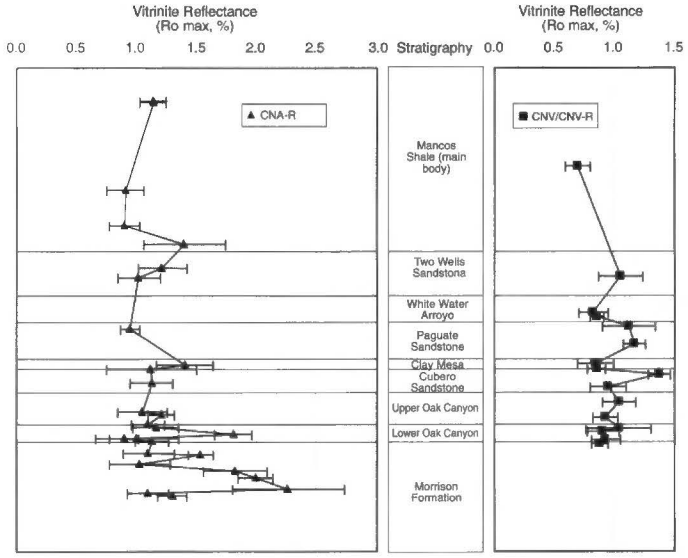

FIGURE 6. Vitrinite reflectance data plotted as a function of depth for boreholes CNA-R and CNV/CNV-R. Error bars are 1 standard deviation. Data for CNA-R have been corrected to reflect true vertical depth. Vitrinite data is from Table 2.

oxidized or weathered vitrinite were not measured. Many of the samples were compositionally very low in organic material, particularly vitrinite. To obtain a sufficient number of readings, in many cases pellets had to be repeatedly polished to obtain fresh surfaces. Samples CNV-R 232.5, CNA-R 1490.0, and CNA-R 1502.0 did not have sufficient vitrinitic material to obtain the desired 20 reflectance readings, even with sequential polishing. The vitrinite readings obtained from these samples comprised 9, 11, and 12 vitrinite readings, respectively. Samples from the vertical boreholes have an average Romax. = 0.97% (n = 16), compared to the samples from the upper part of the angled borehole with an average Romax. = 1.16% (n = 21). Samples in the vicinity of basalt dikes have higher Romax. of 1.58% (n = 6).

Burial/uplift curve

The Dakota–Mancos sequence in west-central New Mexico was deposited over a 6-Ma period (88–94 Ma ago) during Late Cretaceous time (Molenaar and Baird, 1992). Sedimentation in this region probably continued to about 36 Ma (Dickinson et al., 1988). Through regional stratigraphic correlation, the Dakota–Mancos sequence is estimated to have reached a maximum burial depth in this portion of the San Juan Basin of about 1.7 km (Molenaar, 1973, 1983; Molenaar and Baird, 1992). In the center of the basin, Mancos depths exceeded 2.0 km (Law, 1992). Figure 7 shows the estimated burial curves for strata in the Cerro Negro boreholes. Because of uncertainty associated with the extent of Tertiary sediments overlying Cerro Negro, three cases were developed, but only one is shown. The case without significant unconformities in the sequence was judged to be the most plausible and was used for the burial curve shown in Figure 7. The other two cases (not shown) have shallower maximum depths of burial, as shallow as 1.3 km for the case with the least amount of accumulated Tertiary sediments overlying the sequence at maximum depth of burial.

The method used to create the burial curve was that of Sclater and Christie (1980) as implemented in the commercially available software program entitled "Subside! A Basin Analysis Program" (Wilkerson and Hsui, 1989). This program performs backstripping of the sedimentary sequence to establish the burial curve and accounts for decompaction and sediment load removal. To perform the calculations, the full stratigraphic sequence (thickness data) for the region around Cerro Negro

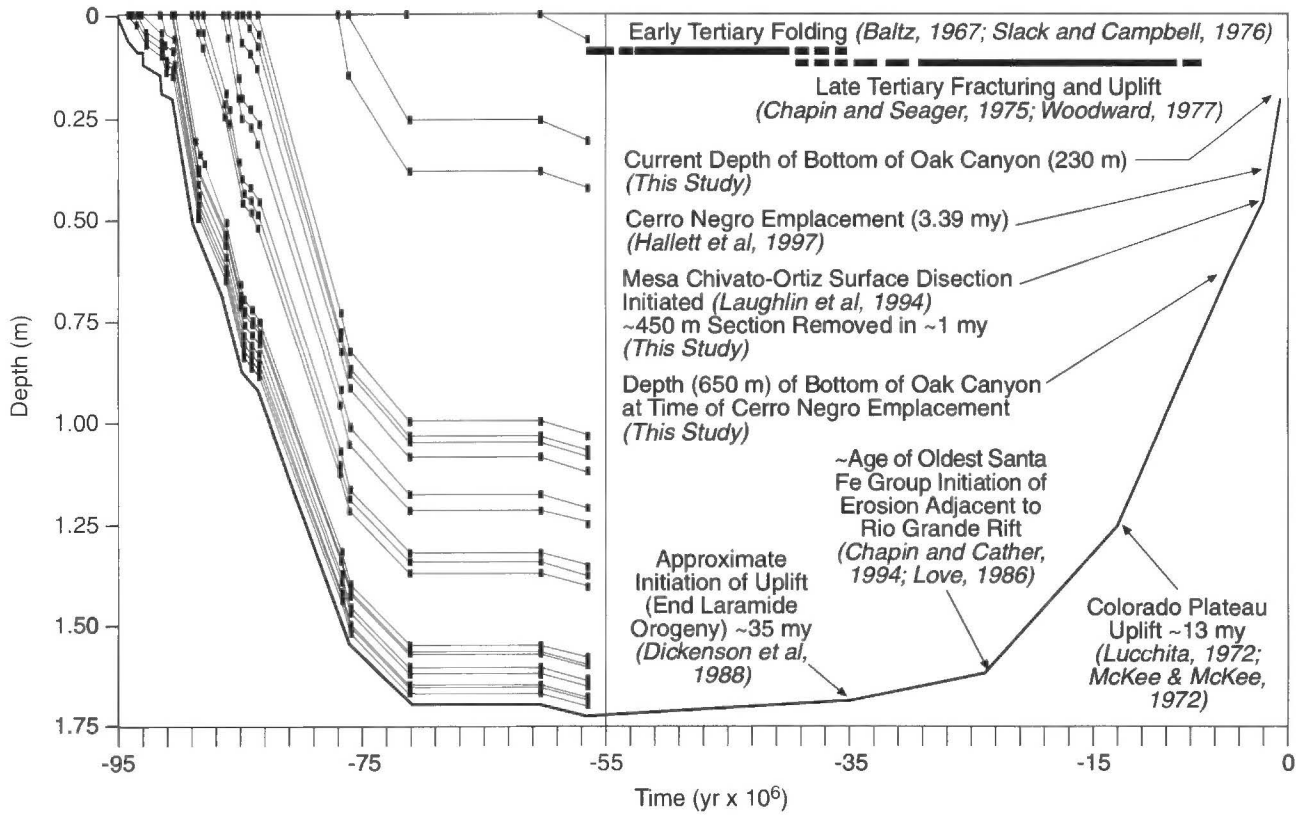

FIGURE 7. Burial and exhumation curves for strata in the vicinity of Cerro Negro. Lower curve on the right side of diagram represents the bottom of the Oak Canyon Member of the Dakota Sandstone. Curves to the left represent successively shallower strata in the Dakota–Mancos sequence. Units and thicknesses used to construct burial curve include: Oak Canyon 31 m, Cubero Sandstone 13 m, Clay Mesa Shale 7 m, Paguate Sandstone 25 m, Whitewater Arroyo Shale 16 m, Two Wells Sandstone 31 m, Mancos Shale 204 m, Gallup Sandstone 24 m, Dilco Coal Member 38 m, Mulatto Tongue 107 m, Dalton Sandstone 38 m, Gibson Coal 88 m, Hosta Tongue 35 m, Satan Tongue 14 m, Point Lookout Sandstone 38 m, Menefee Formation 610 m, Fruitland Formation 122 m, Kirtland Shale 46 m, and Ojo Alamo Sandstone 61 m.

TABLE 2. Vitrinite reflectance data for CNV, CNV-R and CNA-R boreholes (NA-not available).

Borehole	Sample Depth (m)	Distance to Plug (m)	% Reflectance Maximum (Rv max%)	Std Dev. (Rv max%)	% Reflectance Random (Ro %)	Std Dev. (%Ro)	% Reflectance Minimum (Rv min%)	Std Dev. (Rv min%)	Rotational Average	Std Dev. Rot. Avg.	Bireflectance (Rv max%–Rv min%)	Std. Dev. Bireflec-tance	# of measure-ments	Comments
CNV	61.1	1000	0.694	0.107	0.675	0.108	0.638	0.107	0.660	0.107	0.054	0.016	20	Mancos Shale Main Body
CNV	128.5	1000	1.049	0.184	1.009	0.183	0.980	0.175	1.011	0.179	0.068	0.038	20	Two-wells SS (middle)
CNV	151.2	1000	0.825	0.119	0.785	0.110	0.755	0.094	0.783	0.105	0.070	0.038	20	Whitewater Sh (bottom)
CNV	153.8	1000	0.861	0.058	0.829	0.054	0.773	0.062	0.809	0.019	0.086	0.019	20	Paguate SS (top)
CNV	159.1	1000	1.121	0.221	1.098	0.208	1.041	0.179	1.075	0.197	0.079	0.049	20	Paguate SS (upper middle)
CNV	170.9	1000	1.169	0.096	1.149	0.100	1.108	0.089	1.131	0.091	0.059	0.028	20	Paguate SS, shaly (middle)
CNVR	182.5	1080	0.843	0.147	0.809	0.150	0.782	0.148	0.810	0.146	0.061	0.015	20	Clay Mesa Sh (middle)
CNVR	186.3	1080	0.852	0.072	0.828	0.066	0.759	0.098	0.800	0.083	0.092	0.045	20	Cubero SS (top)
CNV	189.3	1000	1.378	0.091	1.243	0.096	1.121	0.099	1.245	0.095	0.256	0.039	20	Cubero SS (upper middle)
CNV	197.0	1000	0.947	0.153	0.921	0.161	0.800	0.140	0.869	0.143	0.145	0.082	20	Cubero (bottom)
CNVR	206.5	1080	1.046	0.14	0.995	0.128	0.976	0.128	1.008	0.134	0.068	0.032	20	Oak Canyon SS-Sh (middle of upper)
CNVR	216.5	1080	0.921	0.104	0.828	0.131	0.814	0.139	0.867	0.118	0.105	0.058	20	Oak Canyon SS-Sh (top of lower)
CNVR	222.9	1080	1.036	0.277	1.001	NA	0.964	NA	0.995	0.266	NA	NA	20	Oak Canyon SS-Sh (middle of lower)
CNVR	224.9	1080	0.908	0.128	0.870	0.133	0.842	0.125	0.870	0.126	0.064	0.022	20	Oak Canyon SS-Sh (bottom of lower)
CNVR	229.9	1080	0.930	0.124	0.903	0.120	0.848	0.121	0.883	0.121	0.079	0.027	20	Oak Canyon SS-Sh (bottom)
CNVR	232.5	1080	0.878	0.070	0.867	0.063	0.778	0.070	0.819	0.066	0.097	0.032	9	Jackpile SS (upper)
CNAR	48.7	374	1.144	0.109	1.133	0.106	1.072	0.112	1.100	0.109	0.071	0.040	20	Mancos Shale Main Body
CNAR	92.9	320	1.141	0.112	1.098	0.117	1.067	0.117	1.100	0.115	0.072	0.034	20	Mancos Shale Main Body
CNAR	201.2	306	0.910	0.157	0.819	0.143	0.728	0.131	0.813	0.138	0.180	0.064	20	Mancos Shale Main Body
CNAR	239.9	229	0.898	0.127	0.862	0.117	0.805	0.107	0.848	0.117	0.092	0.032	20	Mancos Shale Main Body (bottom)
CNAR	258.6	191	1.404	0.341	1.338	NA	1.274	NA	1.333	0.340	NA	NA	20	Two-wells SS (upper 3rd)
CNAR	280.1	165	1.220	0.204	1.177	0.202	1.095	0.166	1.149	0.178	0.123	0.092	20	Two Wells SS (middle)
CNAR	293.9	150	1.024	0.174	0.944	NA	0.912	NA	0.959	0.169	NA	NA	20	Two-wells SS (bottom)
CNAR	345.4	115	0.949	0.083	0.927	0.082	0.870	0.072	0.902	0.076	0.079	0.028	20	Paguate SS (upper 3rd)
CNAR	381.5	96	1.409	0.236	1.368	0.230	1.319	0.228	1.360	0.230	0.090	0.031	20	Clay Mesa Shale (middle)
CNAR	385.1	94	1.128	0.371	1.088	0.348	0.977	0.300	1.042	0.329	0.150	0.102	20	Cubero SS (upper)
CNAR	402.9	77	1.129	0.178	1.088	0.209	1.021	0.197	1.069	0.184	0.105	0.059	20	Oak Canyon (top)
CNAR	424.6	58	1.054	0.208	0.972	0.195	0.945	0.198	0.995	0.210	0.107	0.031	20	Oak Canyon (bottom of upper, shaly)
CNAR	428.2	56	1.210	0.113	1.192	0.108	1.074	0.120	1.128	0.112	0.135	0.075	20	Oak Canyon (top of lower)
CNAR	437.7	48	1.098	0.143	1.069	0.145	1.024	0.133	1.054	0.139	0.072	0.031	20	Oak Canyon (middle of lower)
CNAR	441.7	45	1.166	0.189	1.131	NA	1.101	NA	1.129	0.178	NA	NA	20	Oak Canyon (bottom of lower)
CNAR	449.2	39	1.812	0.152	1.741	0.181	1.700	0.168	1.750	0.134	0.063	0.030	20	Jackpile SS (upper - near dike)
CNAR	454.2	32	1.006	0.344	0.986	0.331	0.917	0.320	0.953	0.329	0.089	0.034	11	Jackpile SS
CNAR	455.5	31	0.901	0.123	0.860	0.114	0.834	0.126	0.862	0.125	0.064	0.028	20	Jackpile SS (near dike)
CNAR	457.8	30	1.138	0.137	1.082	0.141	1.070	0.151	1.100	0.144	0.067	0.022	12	Jackpile SS
CNAR	463.6	26	1.105	0.213	1.029	0.223	0.958	0.162	1.026	0.182	0.146	0.072	20	Jackpile SS
CNAR	465.7	25	1.539	0.101	1.447	0.091	1.361	0.091	1.453	0.099	0.175	0.033	20	Jackpile SS (between dikes)
CNAR	477.2	19	1.026	0.253	0.962	0.227	0.898	0.245	0.958	0.251	0.126	0.034	20	Morrison Fm (siltstone)
CNAR	481.0	16	1.833	0.267	1.552	0.199	1.353	0.185	1.587	0.218	0.479	0.148	20	Morrison Fm (siltstone near 4th dike)
CNAR	490.4	8	1.998	0.146	1.958	0.151	1.746	0.128	1.858	0.134	0.250	0.046	20	Morrison Fm (siltstone)
CNAR	503.0	1	2.272	0.471	1.998	0.467	1.713	0.402	1.998	0.419	0.558	0.792	20	Morrison Fm (sandstone)
CNAR	507.3	-2	1.100	0.173	1.024	0.162	0.989	0.173	1.042	0.172	0.111	0.044	20	Morrison Fm (sandstone)
CNAR	510.5	-4	1.307	0.121	1.254	0.113	1.182	0.097	1.238	0.105	0.125	0.039	20	Morrison Fm (sandstone)

was used (this study; Baars et al., 1988). At the time of initiation of basin sedimentation, the basement is moved to sea level.

The uplift and erosion portion of Figure 7 is much more uncertain than the burial curve, hence the right side of the figure shows only the base of the Oak Canyon Member. The actual rate of uplift is highly uncertain; the underlying assumption for the uplift curve is that significant changes in rate are associated with regional tectonic events during the early part of the uplift curve. Given that assumption, later changes in geomorphology and related information are used to estimate the uplift rate, constrained by the current depth of the bottom of the Oak Canyon. Key elements taken from the literature to construct the uplift curve include: (1) ~36 Ma, end of Laramide orogeny and approximate initiation of exhumation (Dickinson et al., 1988); (2) ~26 Ma, initiation of erosion adjacent to Rio Grande rift (Chapin and Cather, 1994) and initial incision of Rio Puerco drainage system (Love, 1986); (3) ~13 Ma, uplift of Colorado Plateau as evident from downcutting of the Colorado River (Lucchita, 1972; McKee and McKee, 1972); (4) 6.0–5.3 Ma, creation and subsequent incision of Zuni/Ortiz surface (Laughlin et al., 1994); (5) 3.39 Ma, eruption and emplacement of Cerro Negro basalts (Hallett et al., 1997); (6) current depth of Oak Canyon at 230 m below ground surface (this study).

DISCUSSION

Depositional environments

Laminar bedded siltstones and mudstones of the Brushy Basin Member represent floodplain deposits, whereas massive to planar bedded muddy sandstones, indicating a higher-energy fluvial channel, are representative of a braided-stream depositional environment. A detailed petrographic/diagenetic study has not been completed, so a detailed diagenetic mineralogy is only partly known (Gao et al., 1999). Our interpretation is similar to that reached by Bell (1986) in his regional study of the Brushy Basin being deposited via braided streams to a playa lake system.

A local thickening of the Jackpile Sandstone in the Laguna area (>50 m) was influenced by a pre-Dakota syncline (Condon and Peterson, 1986), the north limb of which rises to the north causing a thinning of the Jackpile to 14 m at Cerro Negro. The Jackpile is interpreted to have been deposited in a braided stream environment similar to that of the Brushy Basin but does not have the associated floodplain deposits as evident by the lack of finer-grained siltstones and mudstones.

The intertonguing Dakota Sandstone and Mancos Shale, which lie unconformably above the Jurassic section, are an overall transgressive sequence. According to Vail et al. (1977) and Kauffman (1979), this intertonguing relationship is in response to an eustatic rise in sea level during medial- and late-Cenomanian time. Superimposed on this large worldwide transgression are three minor regressive events that are represented by the Cubero Sandstone, Paguate Sandstone, and Twowells Sandstone tongues of the Dakota. The oldest reported Cretaceous unit in the area is the Encinal Canyon Member of the Dakota Sandstone, identified by Aubrey (1988) as a fluvial to marginal marine sandstone deposited ahead of the advancing Cretaceous seas. A distinct Encinal Canyon Sandstone is not recognized in the Cerro Negro boreholes because the diagnostic basal conglomerate is not present. Other Encinal Canyon features such as crossbedding, discontinuous lenses of gray mudstone, and locally abundant disseminated black carbonaceous material are also common in the Oak Canyon, making it impossible to distinguish the two units in this investigation.

Two different Oak Canyon Member depositional facies are recognized in the Cerro Negro boreholes. The lower Oak Canyon unit contains weakly cemented (calcite) muddy sandstones with occasional high concentrations of carbonaceous fragments and thin layers of coal. These are consistent with a paralic to marginal marine origin (Landis et al. 1973). In this investigation, the contact between the lower and upper units is marked by the first up-section occurrence of a thin, sideritic-oolite-rich muddy sandstone (lower unit) to a very well-sorted, glauconitic sandstone. Maxwell (1982) describes a similar contact in the Oak Canyon, however, it lies within the upper unit not as a contact boundary. The upper calcite cemented and bioturbated muddy sandstones and sandy mudstones are of marginal marine origin. Additional interbedded Mancos Shale tongues (Clay Mesa and Whitewater Arroyo) were deposited in a deep marine environment. Laminar bedding in the lower shales gives way to bioturbated, coarser-grained sediments further up section, which may reflect lowering of sea level.

The three Dakota Sandstone members (Cubero, Paguate, and Twowells) were deposited in a shoreface or wave-dominated, nearshore environment (e.g., offshore bar) as evident from the well-sorted, crossbedded character of these sandstones. In core these sandstones exhibit coarsening upward sequences with shale at the base grading upward to siltstone and sandstone, followed by a sharp boundary with the succeeding marine cycle. Glauconite appears in the better-sorted, sand-rich intervals of the Paguate and Twowells. It is possible this glauconite formed during early diagenesis of fecal matter (Williams et al., 1982)

The main body of the Mancos Shale is a marine transgressive unit deposited on and near the edge of a continental shelf. The cyclic claystone-mudstone-sandstone sediment packages, which repeat at least five times in the upper half of the main body (Fig. 3), are believed to have been deposited on and near the edge of the continental shelf break and are possibly a deep-water signature of small-scale waning regressive cycles. Such packages could be generated at a shelf break, where repeated minor changes in sea level would be amplified and sandstones would represent the shelf or foreslope facies, and finer-grained mudstones and claystones would represent the transition to toe-of-slope facies. In any case, the thick accumulation of mudstone, siltstone, and sandstone above the Twowells represents a significant transgression and deepening of the sea in this area (Seboyeta Bay of Cobban and Hook, 1989) during the late Cenomanian.

Geometry of Cerro Negro

During the drilling of CNA-R, subsurface gyroscopic surveys were conducted to record the directional advancement of the drill bit. Although one objective of the drilling program was to intercept south plug at depth, we never drilled into a large basaltic body (Fig. 8). One explanation for not intersecting a large basaltic mass is that the drill bit wandered too far off course to intercept the plug, although survey data indicate that we should have grazed the south side of the plug (Fig. 8A). Alternatively, there may be no large basaltic body that exists 300 m below the surface expression of south plug as illustrated in Figure 8B. A dense basaltic plug may only exist to a depth in which the volcanic eruption created space (at depth) by removing sedimentary strata through the eruptive process. It is here suggested that the morphology of Cerro Negro at depth may resemble more of a tuff ring then a tuff cone or cinder cone (Heiken, 1971). The latter of these two explanations may reveal something about the formation of volcanic necks in general; it presents a hypothesis that could be tested by further drilling and supported by detailed mapping of other Rio Puerco volcanic necks.

Fractures

Surface mapping clearly indicates a preferred, steeply dipping NNE fracture trend presumably capable of enhancing horizontal and vertical fluid and microbial transport. But, given the evidence that these fractures die out against finer-grained less competent rocks, it is unlikely the NNE fracture set is the dominant flow mechanism in the interfingering shale–sandstone sequence of the Dakota–Mancos. Porous medium flow may indeed be the dominant mechanism of microbial movement in the subsurface near Cerro Negro, however, more subsurface fracture data are required to assess fully this hypothesis.

The NNE joint set is interpreted to have developed in response to Late Cenozoic regional east–west extension. The ESE joint set may represent unsystematic cross joints that have no tectonic significance, however, they are more likely to be a secondary set, formed during uplift and relaxation of the compressive in situ stresses associated with eruption and emplacement of basalts.

Thermal history

One of the primary research goals of this project was to evaluate whether or not the thermal regime at the Cerro Negro site resulted in

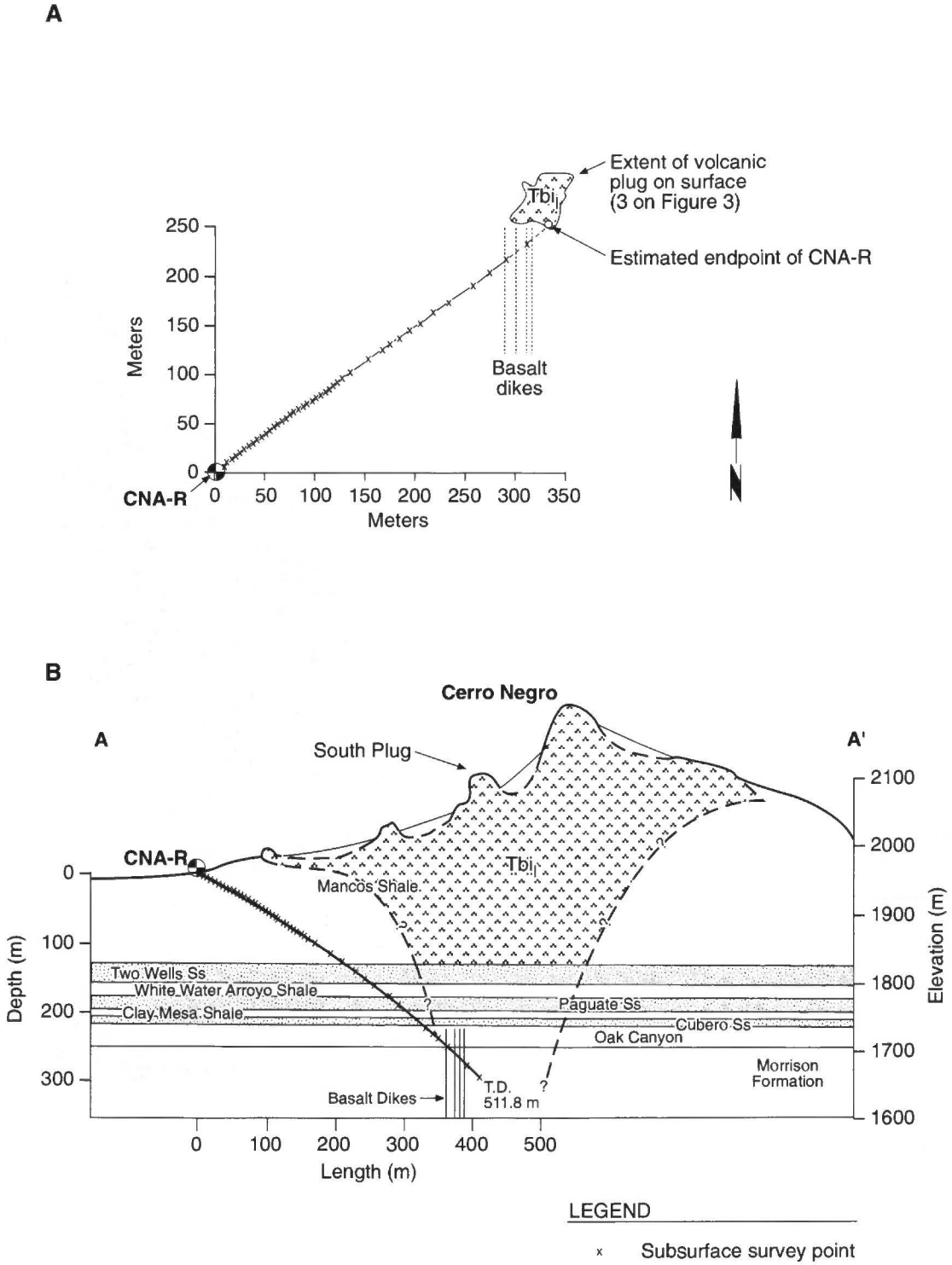

FIGURE 8. Plan view map **A,** and geologic cross section **B,** showing horizontal and vertical drilling azimuths. Subsurface survey points collected with downhole gyroscopic instrumentation.

sterilization of the Dakota–Mancos sequence adjacent to the volcanic neck. If sterilization did occur, then the presence of subsurface microorganisms today in the sterilized zone demonstrates that microbial populations are mobile on a time scale of less than 3.39 Ma. While the exact temperature to which bacteria will survive is controversial, some organisms can survive at temperatures up to 100°C (Stetter, 1986), and this introduces uncertainty regarding sterilization.

The Dakota–Mancos sequence probably reached a maximum burial depth of approximately 1.7 km (Fig. 7). If a 25°C surface temperature and a 25–35°C/km thermal gradient are assumed (Eggleston and Reiter, 1984), then the Dakota–Mancos sequence may have reached a maximum burial temperature of about 85°C, clearly below the temperature of sterilization and consistent within the range of other CNV and CNA-R geothermometers (Gao et al., 1999).

Low $R_{omax.}$ values (0.43–0.53%; Minier and Reiter, 1989) from stratigraphically higher coals in the Colorado Plateau region are in contrast to the high $R_{omax.}$ values (>0.97%) of particulate vitrinite from shale and sandstone samples collected in this investigation from the

Dakota–Mancos sequence. Modeling of our vitrinite reflectance data from Mancos Shale and Morrison sandstone samples suggests a high-temperature regime of about 200°C (Mukhopadhyay and Dow, 1994). Similarly, Elliott et al. (1999) interpret a subset of the vitrinite reflection data to mean that the Dakota–Mancos sequence samples about 1.3 km away from Cerro Negro were heated to 100–125°C. Based on a relative comparison of vitrinite values from CNV/CNV-R and CNA-R, samples within approximately 50 m of the plug are interpreted to have been heated to >125°C. The latter disagrees with other thermal indicators, whereas model temperatures derived from the vitrinite reflectance data of stratigraphically higher regional coals are consistent with low-temperature thermal indicators (i.e., <100°C).

To derive the best scenario for the thermal regime of the Dakota–Mancos sequence at Cerro Negro, Gao et al. (1999) calculated the burial temperatures and vitrinite reflectance data from coals in response to the change of geothermal gradient (Suzuki, 1990). This calculation was carried out with a consideration of thermal constraints provided by mineralogical, isotopic, and fluid inclusion evidence. It appears that a 30°C/km average thermal gradient, or a maximum burial temperature of about 75°C, best explains the present characteristics of all thermal indicators, except vitrinite data from shale and sandstone samples. Two other features of the vitrinite reflectance data are important (Fig. 9): (1) samples within a few meters of one another have very different Romax. values and, (2) samples 1.3 km away from Cerro Negro intrusion have Romax. values inconsistent with lower temperatures of other paleotemperature indicators. We suggest that the close proximity of differing Romax. values is associated with actual maximum temperature variation caused by groundwater circulation during the eruption and emplacement of Cerro Negro. Retrograde impacts to vitrinite caused by the associated moderate- to low-temperature groundwater circulation may also have played a role.

In any case, a relatively low-temperature thermal regime seems to characterize the Dakota–Mancos sequence. Higher temperature excursions, such as caused by volcanic intrusions, may have lasted only a short period of time and thus affected vitrinite, which responded in a different time scale than the smectite–illite transition (Elliott et al., 1999). A short thermal pulse associated with volcanic intrusions is the preferred explanation for the high-Romax. values of shale and sandstone samples, including those in CNV and CNV-R.

SUMMARY

The Dakota–Mancos sequence at Cerro Negro represents a transgressive marine sequence deposited during the emergence of an epicontinental marine basin. Oak Canyon deposits are indicative of a paralic to marginal marine setting. Three sandstone bodies (Twowells, Paguate, and Cubero), which interfinger with Mancos Shale members (Whitewater Arroyo and Clay Mesa), represent either a shoreface or nearshore environment. The thick accumulation of Mancos Shale (main body) is representative of a marine transgressive unit deposited on or near the edge of a continental shelf.

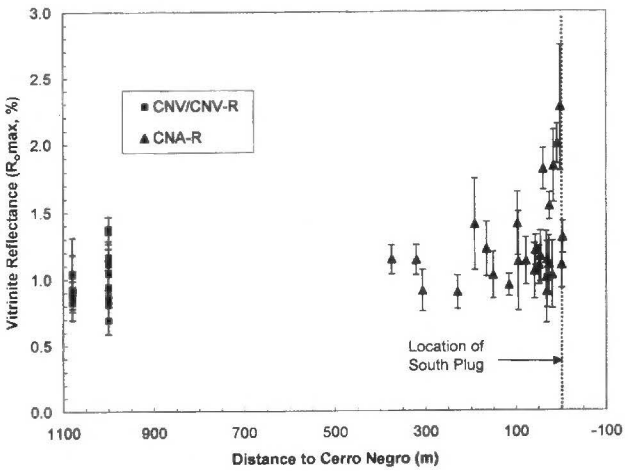

FIGURE 9. Vitrinite reflectance data as a function of distance from Cerro Negro. Error bars are 1 standard deviation.

The five igneous features mapped at Cerro Negro trend at N5°E, a trend similar to one of two local (and regional) fracture trends. Because no large basaltic body was encountered beneath the surface expression of the southern plug, it is possible that the south Cerro Negro plug is morphologically similar to a tuff ring.

Two dominant fracture trends were identified in outcrop and core analyses. The NNE-trending set is predominant. The second set is distributed around a mean trend of ESE and possibly originated during uplift and relaxation of the compressive in situ stresses. Fracture orientations do not vary with distance from the intrusion, however, fracture density does increase towards Cerro Negro. Fracture analyses suggest porous media flow to be the predominant flow mechanism at depth.

The thermal regime of Cerro Negro, based primarily on vitrinite reflectance data, suggest that sandstones and shales within approximately 50 m of the Cerro Negro volcanic necks were sterilized or at least experienced a major reduction in microbial populations. Rocks outside of this zone may have experienced a lesser thermal pulse from Cerro Negro but likely did not undergo sterilization.

ACKNOWLEDGMENTS

This investigation was funded by the U.S. Department of Energy Subsurface Science Program under the guidance of Dr. Frank Wobber. We thank the people of the Cebolleta Land Grant for permission to conduct basic research on their lands. The authors thank G. Hoffman and R. Chamberlin for their reviews.

REFERENCES

Aoki, K. and Kudo, A. M., 1976, Major-element variations of late Cenozoic basalts of New Mexico; *in* Elston, W. E. and Northrop, S. A., eds., Cenozoic volcanism in southwestern New Mexico: New Mexico Geological Society, Special Publication 5, p. 82–88.

Aubrey, W. M., 1988, The Encinal Canyon Member, a new member of the Upper Cretaceous Dakota Sandstone in the southern and eastern San Juan Basin, New Mexico: U.S. Geological Survey, Bulletin 1633-C, p. 58–69.

Baars, D. L., Bartleson, B. L., Chapin, C. E., Curtis, B. F., De Voto, R. H., Everett, J. R., Johnson, R. C., Molenaar, C. M., Peterson, F., Schenk, C. J., Love, J. D., Merin, I. S., Rose, P. R., Ryder, R. T., Waechter, N. B. and Woodward, L. A., 1988, Basins of the Rocky Mountain Region; *in* Sloss, L. L., ed., Sedimentary cover of the North American craton: Geological Society of America, The Decade of North American Geology, v. D-2, p. 109–220.

Bell, T. E., 1986, Deposition and diagenesis in the Brushy Basin Member and upper part of the Westwater Canyon Member of the Morrison Formation, San Juan Basin, New Mexico: American Association of Petroleum Geologists, Studies in Geology, no. 22, p. 77–92.

Bjornstad, B. N., Long, P. E. and Lorenz, J. C., 1996, Fractures adjacent to a Miocene volcanic neck, Cerro Negro, Cebolleta Land Grant, New Mexico: Geological Society of America, Abstracts with Programs, v. 28, p. 49–50.

Brown, W. T., 1969, Igneous geology of the Puerco Necks [M.S. thesis]: Albuquerque, University of New Mexico, 89 p.

Brunton, G. D., 1952, The study of an unusual augite near Cabezon Peak, Sandoval County, New Mexico [M.S. thesis]: Albuquerque, University of New Mexico, 40 p.

Chapin, C. E. and Cather, S. M, 1994, Tectonic setting of the axial basins of the northern and central Rio Grande rift; *in* Keller, G. R. and Cather, S. M., eds., Basins of the Rio Grande rift: Structure, stratigraphy, and tectonic setting: Geological Society of America Special Paper, v. 291, p. 5–26.

Cobban, W. A. and Hook, S. C., 1989, Mid-Cretaceous molluscan record from west-central New Mexico: New Mexico Geological Society, Guidebook 40, p. 247-264.

Colwell, F. S., Stromberg, G. J., Phelps, T. J., Birnbaum, S. A., McKinley, J. P., Rawson, S. A., Veverka, C., Goodwin, S., Long, P. E., Russell, B. F., Garland, T., Thompson, D., Skinner, P. and Grover, S., 1992, Innovative techniques for collection of saturated and unsaturated subsurface basalts and sediments for microbiological characterization: Journal of Microbiological Methods, v. 15, p. 279–292.

Condon, S. M. and Peterson, F., 1986, Stratigraphy of Middle and Upper Jurassic rocks of the San Juan Basin: Historical perspective, current ideas, and remaining problems: A basin analysis case study of the Morrison Formation

Grants uranium region, New Mexico: American Association of Petroleum Geologists, Studies in Geology, no. 22, p. 7–26.

Dickinson, W. R., Klute, M. A., Hayes, M. J., Janecke, S. U., Lundin, E. R., McKittrick, M. A. and Olivares, M. D., 1988, Paleogeographic and paleotectonic setting of Laramide sedimentary basins in the central Rocky Mountain region: Geological Society of America Bulletin, v. 100, p. 1023–1039.

Dutton, C. E., 1884–1885, Mount Taylor and the Zuni plateau: Sixth Annual Report of the U.S. Geological Survey, p. 106–198.

Eggleston, T. and Reiter, M., 1984, Terrestrial heat-flow estimates from petroleum bottom-hole temperature data in the Colorado Plateau and the eastern Basin and Range: Geological Society of America Bulletin, v. 95, p. 1027–1034.

Elliot, W. C., Edenfield, A. M., Wampler, J. M., Mastisof, G. and Long, P. E., 1999, The kinetics of the smectite to illite transformation in Cretaceous bentonites, Cerro Negro, New Mexico: Clays and Clay Minerals, *in press*.

Fredrickson, J. K. and Onstott, T. C., 1996, Microbes deep inside the earth: Scientific American, v. 275, no. 4, p. 68–73.

Gao, G., Onstott, T. C., Long, P. E., Hallett, R. B., Riciputi, L. R., Pratt, L. M. and Feigenson, M., 1999, Diagenesis and thermal regime of the Dakota–Mancos Sandstone/Shale sequence: Constraints on the investigation of subsurface bacteria: Chemical Geology, in review.

Hallett, R. B., 1992, Volcanic geology of the Rio Puerco necks: New Mexico Geological Society, Guidebook 43, p. 135–144.

Hallett, R. B., Kyle, P. R. and McIntosh, W. C., 1997, Paleomagnetic and $^{40}Ar/^{39}Ar$ age constraints on the chronologic evolution of the Rio Puerco volcanic necks and Mesa Prieta, west-central New Mexico: Implications for transition zone magmatism: Geological Society of America Bulletin, v. 109, p. 95–106.

Heiken, G. H., 1971, Tuff rings: Examples from the Fort Rock-Christmas Lake Valley Basin, south-central Oregon: Journal of Geophysical Research, v. 76, p. 5615–5626.

Hunt, C. B., 1937, Igneous geology and structure of the Mount Taylor volcanic field, New Mexico: U.S. Geological Survey, Professional Paper 189-B, p. 51–80.

Johnson, D. W., 1907, Volcanic necks of the Mount Taylor region, New Mexico: Geological Society of America Bulletin, v. 18, p. 303–324.

Kauffman, E. B., 1979, Cretaceous; *in* Robinson, R. A. and Teichert, C., eds., Treatise on invertebrate paleontology, Part A: Geological Society of America and University of Kansas, p. 418–487.

Kudo, A. M., Aoki, K. and Brookins, D. G., 1971, The origin of Pliocene–Holocene basalts of New Mexico in the light of Sr-isotopic and major-element abundances: Earth and Planetary Science Letters, v. 13, p. 200–204.

Landis, E. R., Dane, C. H. and Cobban, W. A., 1973, Stratigraphic terminology of the Dakota Sandstone and Mancos Shale, west-central New Mexico: U.S. Geological Survey, Bulletin 1372-J, 44 p.

Laughlin, A. W., Perry, F., Damon, P., Shafiquallah, M., WoldeGabriel, G., McIntosh, W., Harrington, C., Wells., S. G. and Drake, P., 1994, Geochronology of the Mount Taylor and Zuni-Bandera volcanic fields, Cibola County, New Mexico: New Mexico Geology, v. 15, p. 81–92.

Law, B. E., 1992, Thermal maturity pattern of Cretaceous and Tertiary rocks, San Juan Basin, Colorado and New Mexico: Geological Society of America Bulletin, v. 104, p. 192–207.

Long, P. E. and Wood, B. J., 1986, Structures, textures, and cooling histories of Columbia River basalt flows: Geological Society of America Bulletin, v. 97, p. 1144–1155.

Love, D. W., 1986, A geological perspective of sediment storage and delivery along the Rio Puerco, New Mexico; *in* Hadley, R. F., ed., Drainage basin sediment delivery: International Association of Hydrological Sciences, Publication 159, p. 305–322.

Lucchita, I., 1972, Early history of the Colorado River in the Basin and Range province: Geological Society of America Bulletin, v. 83, p. 1933–1948,

Maxwell, C. H., 1982, Mesozoic stratigraphy of the Laguna-Grants region: New Mexico Geological Society, Guidebook 33, p. 261–266.

McKee, E. D. and McKee, E. F., 1972, Pliocene uplift of the Grande Canyon region—Time of drainage adjustment: Geological Society of America Bulletin, v. 83, p. 1923–1932.

Minier, J. and Reiter, M., 1989, Coal maturation and geothermal history, west-central New Mexico: New Mexico Geological Society, Guidebook 40, p. 127–133.

Moench, R. H. and Schlee, J. S., 1967, Geology and uranium deposits of the Laguna district, New Mexico: U.S. Geological Survey, Professional Paper 519, 117 p.

Molenaar, C. M., 1973, Sedimentary facies and correlation of the Gallup Sandstone and associated formations, northwestern New Mexico: Four Corners Geological Society Memoir, p. 85–110.

Molenaar, C. M., 1983, Major depositional cycles and regional correlations of Upper Cretaceous rocks, southern Colorado Plateau and adjacent areas; *in* Reynolds, M. W. and Dolly, E. D., eds., Mesozoic paleogeography of the west-central United States: Society of Economic Paleontologist and Mineralogists, Rocky Mountain Section, Denver, p. 201–224.

Molenaar, C. M. and Baird, J. K., 1992 Regional stratigraphic cross sections of Upper Cretaceous rocks across the San Juan Basin, northwestern New Mexico and southwestern Colorado: U.S. Geological Survey, Open-file Report, p. 92–257.

Mukhopadhyay, P. K. and Dow, W. G., 1994, Vitrinite reflectance as a maturity parameter: Applications and limitations: American Chemical Society, Washington, D.C., 294 p.

Onstott, T. C., 1994, DOE seeks origin of deep subsurface bacteria: EOS, v. 75, no. 34, p. 385, 395–396.

Owen, D. E., 1982, Correlation and paleoenvironments of the Jackpile Sandstone (Upper Jurassic) and intertongued Dakota Sandstone-Lower Mancos Shale (Upper Cretaceous) in west-central New Mexico: New Mexico Geological Society, Guidebook 33, p. 267–270.

Rautman, C. A., compiler, 1980, Geology and mineral technology of the Grants uranium region 1979: New Mexico Bureau of Mines and Mineral Resources, Memoir 38, 400 p.

Saucier, A. E., 1979, Grants uranium region guidebook: Albuquerque to Ambrosia Lake, New Mexico: Albuquerque, Published privately, 25 p.

Schlee, J. S. and Moench R. H., 1963, Geologic map of the Moquino quadrangle, New Mexico: U.S. Geological Survey, Geologic Quadrangle Map GQ-209, scale 1:24,000.

Sclater, J. G. and Christie, P. A. F., 1980, Continental stretching and explanation of the post-mid-Cretaceous subsidence of the central North Sea Basin: Journal of Geophysical Research, v. 85, p. 3711–3739.

Spry, A., 1962, The origin of columnar jointing, particularly in basalt flows: Journal of the Geological Society of Australia, v. 8, p. 191–216.

Stetter, K. O., 1986, Diversity of extremely thermophilic achaebacteria; *in* T. D. Brock, ed., Thermalphiles-general, molecular, and applied microbiology: John Wiley and Sons, New York, p. 39–74.

Suzuki, N., 1990, Application of sterane epimerization to evaluation of Yoshii gas and condensate reservoir, Niigata Basin, Japan: American Association of Petroleum Geologist Bulletin, v. 74, p. 1571–1589.

Turner-Peterson, C. E. and Santos, E. S., 1986, Overview and summary: American Association of Petroleum Geologist, Studies in Geology, no. 22, p. 1–6.

Vail, P. R., Mitchum, R. M. and Thompson, S., III, 1977, Seismic stratigraphy and global changes of sea level, Part 4: Global cycles of relative changes of sea level: American Association of Petroleum Geologist, Memoir 26, p. 83–97.

Wilkerson, M. S. and Hsui, A. T., 1989, Subside! A Basin Analysis Program, Copyright 1989, First Edition (commercially available software program).

Williams, H., Turner, F. J. and Gilbert, C. M., 1982, Petrography: An introduction to the study of rocks in thin sections: W. H. Freeman and Company, San Francisco, p. 367.

Wilshire, H. G., Meyer, C. E., Nakata, J. K., Calk, L. C., Shevais, J. W., Nielson, J. E. and Schwarzman, E. C., 1988, Mafic and ultramafic xenoliths from volcanic rocks of the western United States: U.S. Geological Survey, Professional Paper 443, 49 p.

Ed Beaumont holding the rapt attention of a group of NMGS field trip participants as he explains the coal deposits of the San Juan Basin on a pre-meeting trip northeast of Torreon prior to the beginning of the 1992 trip. One may do this when the guidebook was dedicated to you as it was to Ed that year (photograph courtesy of George Austin).